Ultra-High Resolution Imaging of Energetic Material Modifiers[1]

Pamela J. Kaste*, Alba Lalitha Ramaswamy° and Michael A. O'Keefe ж

* Army Research Laboratory, Aberdeen Proving Ground, MD 21005

° ECE Department, A.V. Williams bldg, University of Maryland, MD 20742

ж MSD, Lawrence Berkeley National Laboratory B2-200, CA 94720

DISCLAIMER

Ernest Orlando Lawrence Berkeley National Laboratory – LBNL-52384

Ultrahigh Resolution Imaging of Energetic Material Modifiers[2]

Pamela Kaste, Sam Trevino
Army Research Laboratory, APG, Maryland

Alba Lalitha Ramawamy
University of MD, College Park, MD

Michael A. O'Keefe
Materials Sciences Division, LBNL, Berkeley, CA

ABSTRACT

Development of novel energetic materials with improved performance, sensitivity and vulnerability properties requires many years from conception, synthesis, scale-up, formulation & processing, and ultimately, to evaluation. Recent approaches have focused on using modifiers, which might be added at relatively low levels for improving the properties of existing propellant and explosive formulations, or alternatively, might modify existing energetic materials themselves for improved properties.   Research in nanotechnology, aided by advancements in instrumentation for imaging and characterization at the nano-scale, has become an important focus for modification of materials in general. Nanomaterials offer potential for energetic materials, for improving ignition, burning and combustion, and response to initiation phenomena, but exploitation of these materials requires an understanding of their detailed structure that gives them special functional characteristics that make them attractive for materials modification. In this paper, nanoscale imaging, and even sub-nanoscale imaging approaching atomic dimensions has been performed on energetic materials of interest for both explosive and propellant modification. Characterization at the nano-scale level is essential for understanding the unique properties of these materials which serve as a basis to understand how they may react or modify a matrix into which they are embedded.

BACKGROUND

Carbon Nanotubes

Carbon nano-tubes (CNTs) have a unique coiled graphitic structure, and were first discovered in 1991 (Iijima, 1991). They can form with a single cylindrical wall (SWNT) or multi-walls (MWNT). The larger the diameter of the tubes, the more likely they are to be multi-wall; e.g. a 50 nm internal diameter tube typically has up to 6 multi-walls and a 1.2-1.4 nm diameter tube is single-walled. The length and internal diameter can vary significantly depending on production conditions. Thus the typical dimensions of CNTs can vary from 1-100 nm internal diameter and 2-10 µm in length (though tubes up to 2 mm in length have been reported, Pan, 1998). With recent improvements in production conditions, the dimensions and quality of tubes can be well controlled.

The crystal structure of carbon nanotubes has been measured by various techniques and determined to consist of the coiled graphitic structure. Graphite sheets can slide past each other conferring the smooth lubricant properties typical of the material. Tubes with a different chirality or twist have been reported where the lattice parameter, density and interlayer spacing varies

---

[2] Distribution limited to U.S. government agencies and their contractors, critical technology. Other requests for this document shall be referred to U.S. Army Research Laboratory, ATTN: AMSRL-WM-B, APG, MD 21005-5066, March 2003.

(Gao, 1997). The Young's modulus of elasticity for single-wall CNTs has been found tobe close to 1TPa with a maximum tensile strength close to 30 GPa (Yu, 2000; Schewe, 1996). There are variations in the reported values, measurement techniques, sample orientation and calculated values. The research is ongoing.

The electrical conductivity along their length can be very high, reaching stable current densities of up to 10^{13} Ω/cm^2 (Frank, 1997; Yakobson, 1997), which corresponds to 120 billion to 3 trillion electrons per second; in comparison, a typical 18-gauge copper wire carries a current density of up to 10^2 Ω/cm^2 (Ellenbogen, 1999). The CNTs have thus been considered as the "nano-wires" of future molecular computers where the individual diodes and transistors are considered to be built from single organic molecules combined and doped appropriately. The conductance has been found to be quantized (Sanvito, 1974; Frank, 1998; Dekker, 1999) and to vary according to the chirality of the tube. Thus the CNT has the ability to be metallic or semi-conducting depending on the twist of the tube (Wilder, 1998).

Finally the thermal conductivity is reported to be about 2000 W/m/k (Che; Hone, 1999; Berber, 2000), which approaches that of diamond. However there is still a lot of controversy on the actual thermal conductivity and its temperature dependence. The purity of carbon nanotubes is critical in determining their thermal stability. When heated in a thermogravimetric analyzer (TGA), CNTs produced by NanoLab (Brighton, MA), which are about 96-98% pure, decompose between 450-500 ˚C. The main contaminants are silicon and nickel catalyst, which come from the production process. Some amorphous carbon is also present. CNTs from other sources burn at around 250˚C but have a 15% residual catalyst impurity. Since the catalyst remains as a tip on the nanotube, most can be removed through an acid-etching process.

The standard CNT fabrication process consists in sputtering a nickel catalyst onto the surface of a substrate, which can consist in molybdenum, titanium, graphite, quartz, silicon, alumina. The substrate is heated to 600-800 ˚C in the presence of a DC plasma, where acteylene and ammonia gases are introduced. The acetylene decomposes and diffuses through the catalyst and crystallizes as a nanotube on the substrate. For nano-arrays, application of an electric field during growth aligns the tubes.
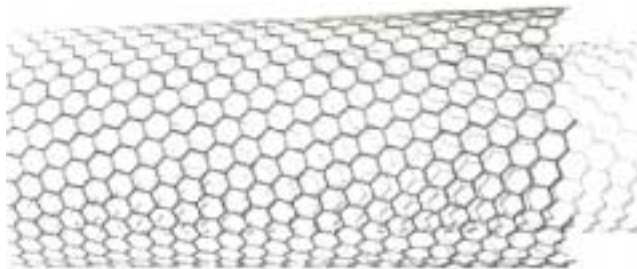

Figure 1. Schematic of a Carbon Nanotube.

The coiled graphitic structure of carbon nano-tubes (CNTs) shown in Figure 1, confers unique properties to the nanotubes. The longitudinal tensile strength is reported to be up to one hundred times that of steel (Pan, 1998). Because the diameters of CNTs are nano-scale while their lengths can be micro-scale, they also have exceedingly high aspect ratios. This offers the potential for achieving a maximum effect with a minimum of level of parasitic material. Such properties make nanotubes attractive as a new candidate ingredient for propellant formulations with the potential for improving the ignition and combustion properties. Moreover, since the tubes consist of pure carbon, they pose no adverse effect to the environment.

Through the use of carbon nanotubes it may also be feasible to enhance the specificity of a propellant formulation to initiation by plasma, due to the high electron density and conductance localized on the nanotube walls. Stability, which is a property that is generally diametrically opposed to reactivity, may be augmented by encapsulation of nanoenergetic materials within the carbon nanotube. The carbon nanotube encapsulation technology has the potential for providing safer and more efficient handling and compaction of energetic materials by facilitating insertion and packing into the formulations. Methods for preparation of energetic crystals of nanoscale dimensions and methods for insertion into the tubes are technology efforts that are being developed and investigated.

Studies are being performed to assist in the research effort to incorporate/bind the carbon nano-tubes within propellant matrixes, and to understand their effects on the initiation, performance, safety and mechanical properties of formulations containing them. A key to the effectiveness of nanotubes will be in the ability to thoroughly disperse them in the propellant matrix. One approach to increase the affinity of the tubes for energetic binders is to functionalize the tubes. Ultimately derivitization with energetic groups is desired, but an initial approach is to prepare a nanotube precursor which can undergo further reaction with monomers so that a polymer-substituted carbon nanotube is obtained.

Nano-scale modification of propellants with extended structures such as carbon nanotubes is of interest for tailoring the burning rate of propellants for co-layered charge designs which require a nominal burning rate differential of a factor of 3 in order for performance gains to be realized. Since nanotube structures can vary significantly, correlation with performance results requires quality control of the nanotubes being used. In using nanotubes in polymers for commercial applications, it was found that achieving uniform dispersion can be problematic due to the lack of affinity of the carbon structure for polar functional groups. An approach to improve dispersion is to modify the carbon structures with oligimers containing functional groups that will associate with those of the polymer of interest, and that will facilitate incorporation of the nanotube, much the way surfactants are used to bridge polar and non-polar species. Functionalization of carbon nanotubes is being pursued at ARL, and the high resolution imaging of nanotubes that have been modified with several different polymers has been performed.

Nanoscale and Ultra-fine Aluminum Oxide

Aluminum oxide is of great interest for explosives applications, and especially recently, nano-aluminum is a major focus of research for thermobaric applications. Mechanisms controlling the effectiveness of nano-aluminum in modifying explosive properties is not well understood, but it is becoming increasing clear that the particular structural characteristics of the nano-aluminum are key to understanding and controlling not only it's performance but sensitivity and vulnerability properties as well. The properties of the oxide passivation coating, including chemical structure and purity, thickness, and physical & crystallographic structure are important in analyze, understand and control. Ultra-high resolution images of the nano-aluminum structure will be presented, and possible implications of this structure for explosive properties will be discussed.

Bulk aluminum is covered with an extremely thin oxide coating, which is considered to be non-porous and protects it from further oxidation. Typically this oxide coating is no more than 10 nm thick. The role of the oxide coating during the melting and ignition of micron-sized aluminum particles in propellant combustion is not fully understood and has often been considered as a potential "barrier" to reaction. The effects and interaction of the binder and oxidizer combustion on the melting and ignition of the aluminum particles are yet to be fully unraveled. The study of nano-Al particles can provide a better understanding at the "atomic level" of the above phenomena. This understanding can be important both in the use of the standard aluminum and in the tailoring of nano-Al with improved properties for use in propellants and other applications.

Standard micron-sized aluminum used in propellants produces a higher temperature of combustion products and thus increased velocity of gas flow from a rocket motor resulting in a

greater specific impulse. It also raises the density of the grain and alleviates certain combustion instabilities by quenching the acoustic resonant oscillations forming in rocket motors, which would otherwise lead to the structural damage of the motors during flight. However concerns about micron-size Al have arisen in the rocket community: 1) Does the observed agglomeration of micron-sized aluminum on the surface of the propellant impede the combustion process and slow the burning velocity?; 2) Is the combustion of the metallic particles incomplete, and if so, is the oxide coating present on the aluminum surface a factor?; 3) Do condensed oxide combustion products or slag form, and result in a reduction of motor efficiency?.

Nano-Al is being considered as a potential solution to these questions. The approach in this effort is to study nano-Al at the atomic level to begin to understand fundamental phenomena such as surface oxidation, impurity level and distribution, and thermal decomposition and reaction. Work in these areas is in progress, with the goal of better understanding the role of aluminum fuel in propellant combustion and as a component of MICs (Metastable Intermolecular Composites) and thermobaric formulations.

EXPERIMENTAL

Samples

Nanotube samples were provided by NanoLab of Brighton, MA. Typical conditions for the synthesis of nanotubes-polymer hybrid materials are described in the two following procedures (Bratcher, 2001).

The nano-Al sample examined is from the NAVSEA-IH nano-aluminum manufacturing facility, standard batch no. AL-1030-00-1.

High Resolution Microscopy

Carbon nano-tubes were examined with a high-resolution electron microscope JEOL (Japan Electron Optics Limited) Model 1200 EX-2 with the microscope set for the high-resolution transmission mode. The carbon nano-tubes were placed in 100μl of water inside a small test-tube and dispersed by agitation of the tube in a vortex mixer for 10-20 seconds. This allowed the individual tubes to separate for examination under the microscope. Various magnifications were used to image both the individual tubes and the cluster agglomerates.

The nano-Al particles were examined at a resolution of 1.6Å using the NCEM (National Center for Electron Microscopy) Atomic Resolution Microscope (ARM). The microscope was used at an electron energy of 800 keV and magnification of 600 kX to ensure adequate electron beam penetration of the whole (i.e. non-sectioned) nano-Al particles. The electron micrographs obtained were analyzed by computer *a posteriori* imaging, which enabled computer enlarging of selected areas.

Image simulations from model structures can be used to confirm image interpretation of high-resolution electron images (O'Keefe, Buseck & Iijima, 1978). Simulations have shown that atomic characterization at resolutions below 1Å is possible with the NCEM OÅM (One-Ångstrom Microscope), a modified mid-voltage (300kV) microscope using focal-series reconstruction (O'Keefe et al, 2001). Although interpretation of the positions of atom planes can be problematic even at resolutions as good as 1.6A (Malm & O'Keefe, 1997), experiments with the 0.8Å-resolution OÅM have shown that atomic resolution can be achieved in nanoparticles (O'Keefe, Nelson & Allard, 2003). In addition, experiment and image simulations confirm that the OÅM's improved resolution gives it the ability to image all atoms present in the specimen, from the heavier metal atoms to the lighter oxygen, nitrogen and carbon atoms (Kisielowski et al, 2001).

Atomic Force Microscopy was performed at the Army Research Laboratory with a VEECO Metrology (formerly Digital Instruments) Dimension 3100 atomic force microscope with Nanoscope Illa controller, Phase-DO1 external electronics in tapping mode with silicon TESPW probes.

Prompt Gamma Activation Analysis was performed using the spectometer located at the Materials Science and Engineering Laboratory of the NIST Center for Neutron Research in Gaithersburg, MD using neutron guide NG-7. Characteristics of the instrument include an Li-6 glass collimator and antimony-free lead for gamma shielding; the neutron beam filtered through Bi and Be at 77 K. The maximum beam area is 50 mm x 50 mm. The apparatus is controlled and data are acquired through an Ethernet-based ADC-MCA and workstation. An automatic sample changer will be added in the future. The counting system is designed to handle multiple gamma detectors with Compton suppression.

PGAA analysis has wide application for identifying and quantifying many elements simultaneously in samples ranging in size from micrograms to many grams. The sample is continuously irradiated with a beam of neutrons. The constituent elements of the sample absorb some of these neutrons and emit prompt gamma rays that are measured with a high-resolution gamma-ray spectrometer. The energies of these gamma rays identify the neutron-capturing elements, while the intensities of the peaks at these energies reveal their concentration. PGAA is a non-destructive method, and since the chemical form and shape of the sample are relatively unimportant, sample preparation is minimal. Measurement times range from few minutes to several hours per sample. Normally, the sample does not acquire significant long-lived radioactivity, and the sample may be removed from the facility and used for other purposes.

RESULTS and DISCUSSION

The morphology of the CNTs is very important in characterizing their strength or mechanical properties. The CNTs can come in different morphologies: the "bamboo" or platelet-type (which can have a periodic appearance of conical –shaped layers within each bamboo segment (Lee 2001) or the perfect tube. Also, the CNTs when first grown, typically have a hemispherical "cap" at each end. The caps contain 5-membered carbon rings, which are hence strained and can be etched or removed by the action of dilute nitric acid. The "bamboo" or "stacked cup" morphologies consist of chemical termination of dangling carbon bonds at the end of each platelet or cup with carboxyl (COOH) groups. Thus under the action of mechanical stress the line of weak bonding between the "platelets" or "cups" can break open. The perfect carbon nanotubes instead are very strong. Different functional groups can be attached through the COOH groups. This can be done for all CNT types. The advantage of the "bamboo" type (shown in Figure 2) is that functional groups can be attached through carboxyl groups all along the length of the tubes (shown schematically in Figure 3 & 4) rather than just at the ends.

Figure 2. Detail of TEM Micrograph (> 50 Kx) of CNT Showing Repeating Bamboo Structure.
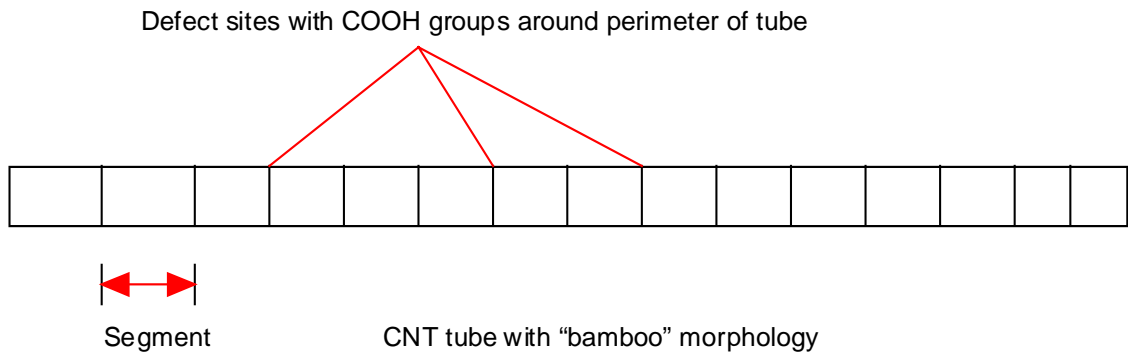
Defect sites with COOH groups around perimeter of tube

Segment

CNT tube with "bamboo" morphology

Figure 3. Schematic of Carbon Nanotubes Illustrating Repeat Structure at Which Sites of Reactivity are Located .
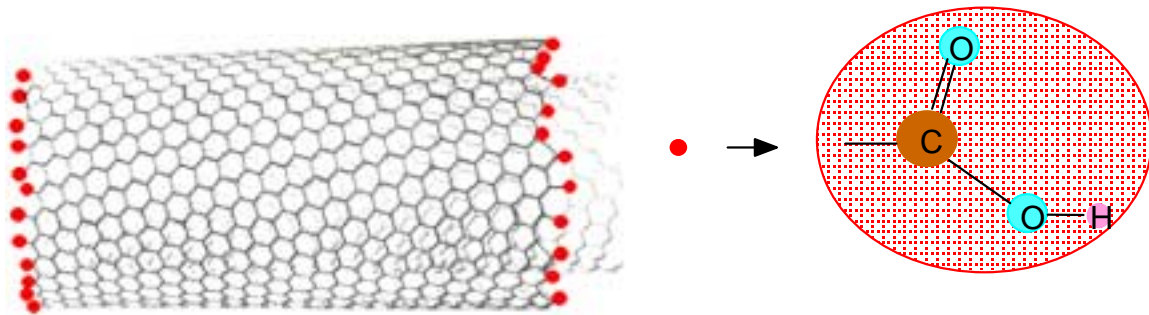
Figure 4. Schematic of Carbon Nanotubes Illustrating Repeat Unit and Carboxylic Acid Defect Sites.

Studies are being performed to assist in the research effort to incorporate/bind the carbon nano-tubes within propellant matrixes, and to understand their effects on the initiation, performance, safety and mechanical properties of formulations containing them. A key to the effectiveness of nanotubes will be in the ability to thoroughly disperse them in the propellant matrix.   One approach to increase the affinity of the tubes for energetic binders is to functionalize the tubes. Ultimately derivitization with energetic groups is desired, but an initial approach is to prepare a nanotube precursor, which can undergo further reaction with monomers so that a polymer-substituted carbon nanotube is obtained.

Figures 5 shows the high-resolution electron micrographs of the unmodified carbon nanotubes magnifications of about 20,000x. The morphology of the tubes is the "bamboo" structure with clear surface features or defects occurring at regular intervals of about 20-60 nm. As can be seen from the micrographs, the tubes are distinct with a clear center core and a 'thick' outer wall. The outer wall actually consists of a series of graphitic layers, forming a multi-wall structure. There are typically of the order of six to nine layers, as determined from transmission electron microscopy of microtomed slices of the carbon nano-tubes. The lengths of the tubes are on the order of 20 μm, while the average diameter is approximately 20 nm. There are variations in tube structure. Some lengths have developed straight, while others are spiral. There is also variation in the size of the tubes, as indicated by the values summarized in Table 1. The data were generated by measuring the structural dimensions of a large sample of carbon nanotubes as examined from high-resolution electron micrographs. The "repeat defect distance" referred to in the table is the size of the segments in a single CNT as depicted in Figure 3. What is very noteworthy is the lack of amorphous carbon in the micrographs, in agreement with the thermal analysis results that are evidence that the tubes are very pure.
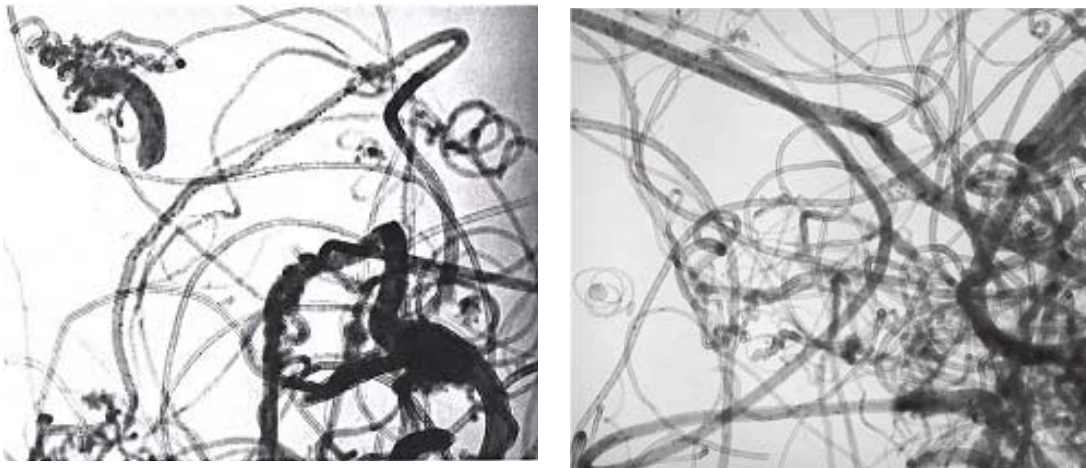

Figure 5. High-Resolution Transmission Electron Micrographs of Unmodified Carbon Nanotube (20,000x).

TABLE 1. Structural and Physical Dimensions of the Carbon Nanotubes.

Structural dimension	Range (nm)	Distribution Modes (nm)	No. of CNTs sampled	Mean (nm)
Inner core diameter(I.D.)	1.25 - 50	2.5, 6.5, 10.5	153	6.25 ± 1.25
Wall thickness	0.625 – 37.5	2.5, 6.9, 10.0	139	5.0 ± 0.5
Outer diameter (O.D.)	2.50 - 85.7	12.50,18.75,25	153	19.0 ± 2.0
Repeat defect distance*	20 - 65	n/a	12	43.0 ± 1.0

The presence of the carboxylic acid sites, available for modification, has been determined by titration (Bratcher, 2001). The carbon nanotubes were functionalized at these carboxyl sites with PMMA to determine reactions and methodology for modification (Figure 6). The line of weak hydrogen bonding between the platelets of the bamboo structure can be opened by the action of mechanical stress. The nature of the PMMA attachment to defect sites in relation to the rest of the tube is very important. Some of the PMMA is attached to the surface of the tube through reactions with the carboxylated defect sites, however, there is also evidence of PMMA around and detached from the tubes. In order to characterize the structure of modified CNTs, it is planned that a gold atom or gold micro-sphere will be attached to each functional group through a sulphur atom. In this way the tubes can be viewed with the high resolution electron microscope and the location of the amine groups can be detected; prompt gamma activation analysis (PGAA) analysis, sensitive to the gold atoms, can then be performed to accurately determine the number of attached functional groups and thus if all defect sites have reacted.

Figure 6. High-Resolution Transmission Electron Micrograph of PMMA-Modified Carbon Nanotube (20,000x).

Experiments performed by Nanolab have shown that under some conditions of mixing, the carbon nano-tubes tend to break at the "bamboo" junctions. However, conditions of mixing for which the stresses do not break the tubes are being investigated. The structure of a carbon fiber is shown in Figure 7.
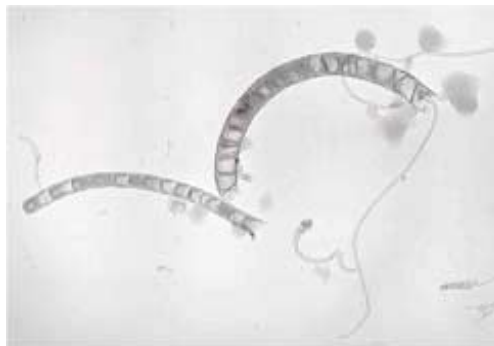

Figure 7. High-Resolution Transmission Electron Micrographs of Unmodified Carbon Nanotube (20,000x).

Prompt gamma activation analysis (PGAA) of NanoLab CNTs was used to determine a C/H ratio of 600:1. From known carbon-to-carbon bond distances (See Figure 8) and the fact that defect sites occur at regular intervals, the defect density can also be computed from PGAA data. The computation can be done accurately through a computer code. A rough estimate was obtained as follows: It is assumed that each carboxyl group is attached to a 6-membered carbon ring at the tube termination. (This is only an approximation since there can be 5-membered rings.) Since each carbon atom in "bulk" is shared by three other carbon atoms, except at the ends of the tubes, each hexagon in the "bulk" contains an average of two carbon atoms. If n is the number of hexagons, a row contains ($2n+2$) carbon atoms, and each "row" is bonded to two hydrogen atoms. The ratio of carbon to hydrogen atoms can therefore be approximated by:

$$C/H \ . \ (2n+2)/2 \ = n+1$$

Given that the ratio of carbon to hydrogen atoms is 600:1, 2.45 Å x 600 (i.e. 147 nm) would represent the average repeat defect distance. The actual repeat distance for defects was measured from micrographs is only 20-60 nm. While this may be due in part to some chirality or twist in the tubes as depicted in Figure 9, or that there are more 5-membered rings than expected, or that the inner tube contains a lower density of defect sites, it is most likely due to the fact that the measured values were made on select tubes with regular defects, while PGAA was run on a bulk sample (no discrimination between types of tubes).
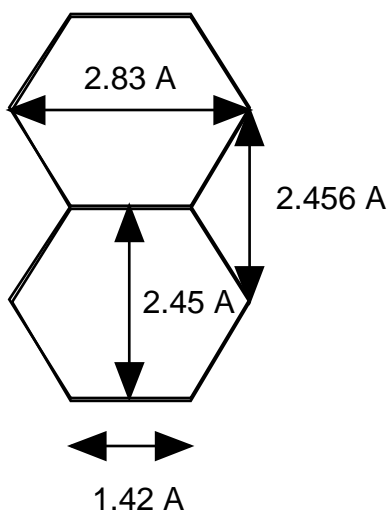
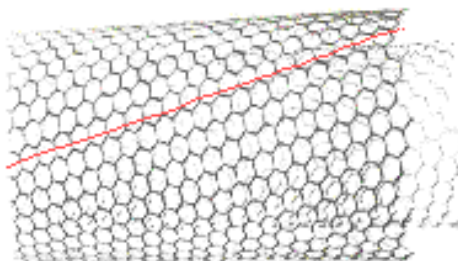

FIGURE 8. Distances of Carbon Atoms in CNT.

FIGURE 9. CNT Structure for C /H Ratio Showing Line Through a Row of Six-Membered Rings and the Twist or Chirality that may Exist in CNTs.

Bulk versus isolated sampling can also yield quite different images. Figures 10 and 11 show the atomic force micrographs for the unmodified- and PMMA-modified CNT samples respectively. The transmission electron micrographs are repeated here for a direct comparison. Samples for each technique are prepared quite differently. For electron microscopy, it is necessary to separate the individual tubes sufficiently so that they don't appear as a dark, un-interpretable clump. Thus, techniques, such as sonication, are used to disperse the nanotubes, and the material that breaks away from the bulk may not be representative. On the other hand, the AFM samples must not vibrate as a small tip is scanned or tapped across the sample. Since adhesives are not convenient to use for this, it is much easier to sample the bulk material. As seen in the AFM image in Figure 10b, the nanotubes that are rather "matted" together yield the best result. The whitened-out areas of the image are actually tubes that have moved during the scan; these usually are tubes that are lying alone or on top; they are often large too.

For the plain nanotubes, although the images look much different, the features that are evident in each are really very similar. They both reveal a range of diameters and lengths, and in each case, some of the smaller tubes appear curled. Note that there is no trace of amorphous carbon in the AFM images either.

For the case of the PMMA-tubes however, the TEM and AFM images are quite different. Although both images show that significant PMMA is present, the distribution of the PMMA appears different. The TEM shows that there is some bulk PMMA present, and at least some of it is attached to the nanotubes; however, most of the nanotube surfaces are free from the PMMA. The AFM images show quite a different phenomenon. In this case the bulk of the material appears to be PMMA with the nanotubes densely embedded within, reminiscent of peanuts in a brittle candy. Examinations of the larger tubes show that they have a very thin coating, such that the original segmentation of the tubes is still apparent. Some of the smaller tubes can be observed embedded in the curled position. The synthesis of the PMMA-modified samples involves reaction of the nanotube with PMMA monomer, so that polymerization actually occurs on the tube (as opposed to attaching a pre-made polymer to the tube). It is unknown at this point how much of the PMMA is attached to the nanotubes, and how much has polymerized independent from the tubes, but in a manner that coats the tubes. Methods of characterization and separation of polymer-modified CNT's from extraneous polymer are currently under consideration.

Both the TEM and AFM data provide valuable information. The TEM is needed to achieve the detailed structural information, and because individual tubes of the polymer-modified sample can be isolated, it is possible to determine that indeed the PMMA is attached to the nanotubes at specific, identifiable locations. The AFM provides visualization of the bulk material and the extent to which the tubes are physically immersed, which would not be easy to achieve with the TEM because that region of the sample would probably appear as a dark blob. Normally, to overcome this problem in TEM, a piece of the sample would be thin-sectioned with a microtome. It is noted that the physical nature of the PMMA sample is much like a very fine powder and is not amenable to microtoming. Dispersion into a matrix such as epoxy for microtoming may be feasible (assuming the embedding process did not disturb the original PMMA-CNT structure), but would be much more laborious and it may be difficult ultimately to differentiate between PMMA and epoxy, assuming the embedding process did not disturb the original PMMA-CNT structure.

a   **b**

Figure 10. a) High-Resolution Transmission Electron Micrograph (40,000x), and b) Atomic Force Micrograph ($5\mu^2$) of Unmodified Carbon Nanotubes.

a   **b**

Figure 11. a) High-Resolution Transmission Electron Micrograph (40,000x), and b) Atomic Force Micrograph ($3\mu^2$) of PMMA-Modified Carbon Nanotubes.

Nano-Energetic Encapsulation

Finally, a technique for encapsulation of energetic particles in the carbon nanotubes has been investigated, including methodology for obtaining nano-scale energetic crystals and their incorporation into nanotubes. The concept is shown schematically in Figure 12. Details cannot be presented at this time, but will be available in the near future. Nanotubes are commercially available in an array form (Figure 13), which offers benefits for many applications. Nanoenergetic crystalline materials embedded into nanotubes offer potential for ignition and burning rate modification needed for novel charge designs in high performance concepts. Such arrays have been thus far evaluated with nano-aluminum particles, which show through the tube walls in high-resolution electron microscopy analysis. The individual carbon nanotubes can be removed from the array substrate by etching.
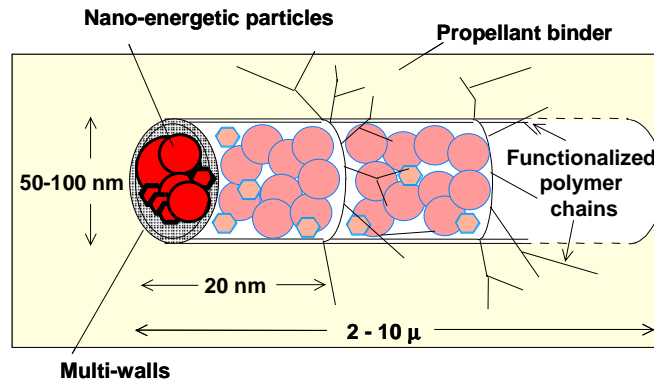
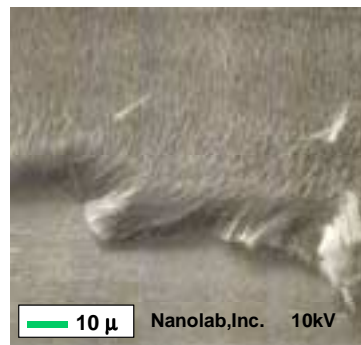**Figure 12. Concept for Nanotube Encapsulation of Energetic Particles.**

Figure 13. Carbon Nanotube Array.

Nano-Aluminum

High-resolution transmission electron microscopy of nanoparticles of aluminum has revealed an amorphous oxide or hydroxide coating about 2.5 nm thick (Figure14a and b), intermixed with single molecular sheets of the oxide/hydroxide. These laminar sheets tend to form prevalently on the surface, and appear to have a different crystalline structure than the underlying layers. This is evident in Figure 14a. Note also the ordered structure of the crystal lattice (which agrees with X-ray results, Witt, 1967) of Al in the bulk matrix, as opposed to the less-ordered structure of the 2.5 nm coating. It may be that the crystalline mismatch causes the outer later to exfoliate, as Figure 14b suggests. Fused particles with distinct grain boundaries are apparent, as Figure 14c shows.

These results are currently being evaluated in conjunction with results of X-ray, thermal and Prompt Gamma Activation analyses, in order to propose a model for the structure and response to thermal initiation of nano-Al, and how that may differ from micron-scale Al.   PGAA measurements have shown that the coating consists of aluminum hydroxide, especially for samples where humidity has come into contact with the material. PGAA analysis has also revealed the presence of B and water. This is in addition to Fe, Cu, N and K impurities evidenced by XPS (Hooton, 2002). It is likely that many of these impurities reside within the coating. No major deformations of the crystalline lattice are observed. PGAA data have also confirmed that the nanoaluminum had absorbed more water than ultrafine aluminum. This may be due to a more porous molecular structure of the coating of nano-aluminum as compared with the ultrafine aluminum. Purity of the Al and the effect on decomposition is of particular interest, as impurities may lower decomposition temperatures of the lattice and affect decomposition behavior and material performance.

Prior experimental observations of the standard micron-sized aluminum include microscopic studies of partially burned or heated samples, visual and photographic observation of the burning, spectroscopic observations of the flame, and collection and observation of the reaction products (Price, 1984). When the micron-sized aluminum particles are heated on a hot stage microscope there is little response until the melting point of 660˚C is reached. The thermal expansion becomes visually evident prior to the melt. When heating is continued in inert atmospheres, the oxide skin breaks open and releases the liquid aluminum, which fuses with that of the neighboring particles to form aggregates (Price, 1984, Crump, 1969). In an oxidizing atmosphere healing of the cracks by the different gases occurs. The oozing out of liquid aluminum followed by aggregation thus takes place at higher temperatures. Evidence of crack healing comes from recovered particles which show expansion crack patterns in the oxide "healed up" by oxidation of the emerging metal (Price, 1984, Crump, 1969). Most of the particle ignition occurs in the flame and takes place in 1-50 ms (Zarko, 1998). The oxide coating is commonly thought to impede or slow the oxidation reaction. However, more detailed experimental studies of the nano-Al, combined with atomistic models are being evaluated to assess if, in fact, the oxide-containing outer layer may contribute to the decomposition of nano-Al. The theoretic work is based on the crystalline structure of aluminum and the potential for single atoms of oxygen to impregnate the Al, possibly resulting in a lower decomposition temperature. This work will be reported in the Proceedings of the 31st International Annual Conference of the Fraunhofer-Institut für Chemische Technologie (Ramaswamy, 2003, submitted).

The AFM provides information regarding bulk material characterization, and results for the NAVSEA-IH nano-aluminum are shown in Figures 15a and b. It is apparent that the NAVSEA-IH nano-aluminum has a very spherical structure and narrow particle size distribution, with nominal particle sizes ranging between 60 and 70 nm. In comparison, ultra-fine flake Al particles are much larger (see Figure 16 for which the 1 µ size area shows only a section of a single particle). The particle itself however seems to have many nanoscale sub-units that have fused together.
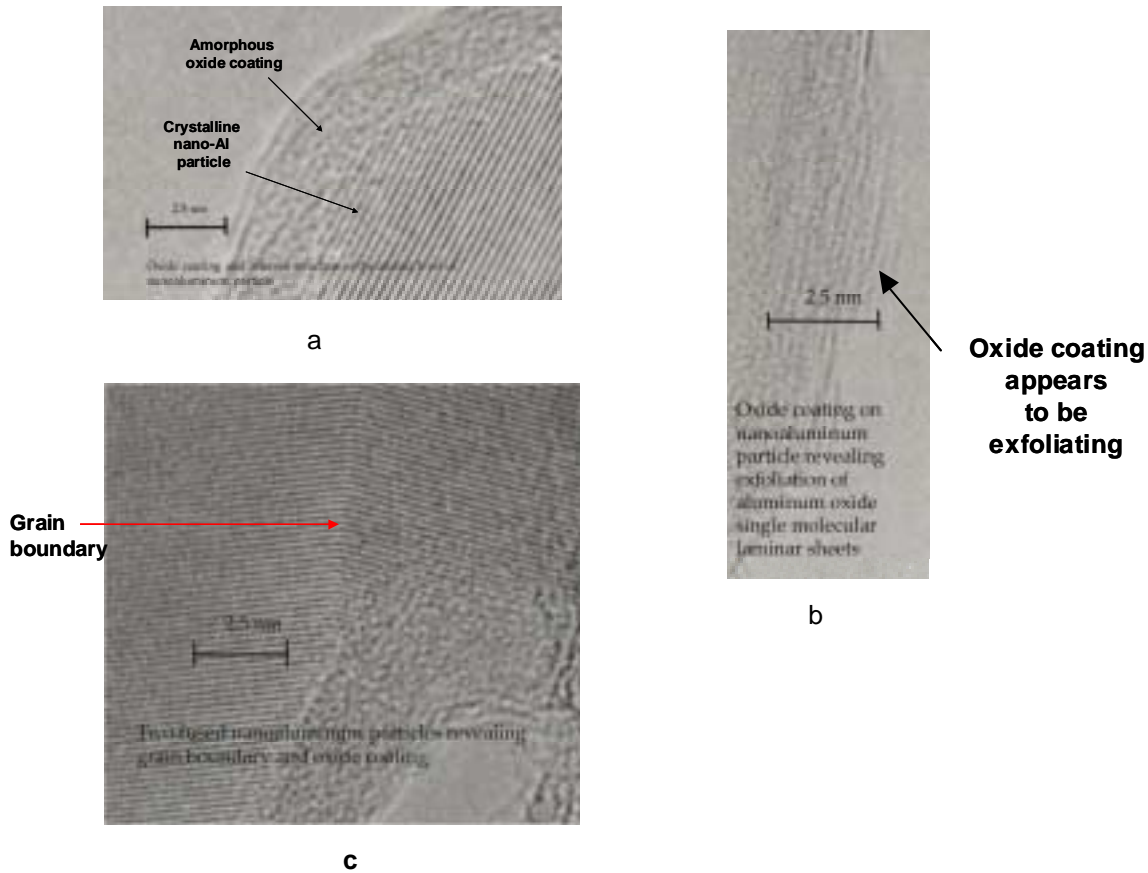
a

b

**Oxide coating
appears
to be
exfoliating**

c

Figure 14. Nano-Aluminum Imaged with an ARM-1000 Microscope:
a) the outer area of a nano-particle of aluminum showing the different morphology of the internal Al crystalline matrix and the ~2.5 nm oxide coating; b) the oxide coating appears to be exfoliating; c) the grain boundary between two fused Al particles.
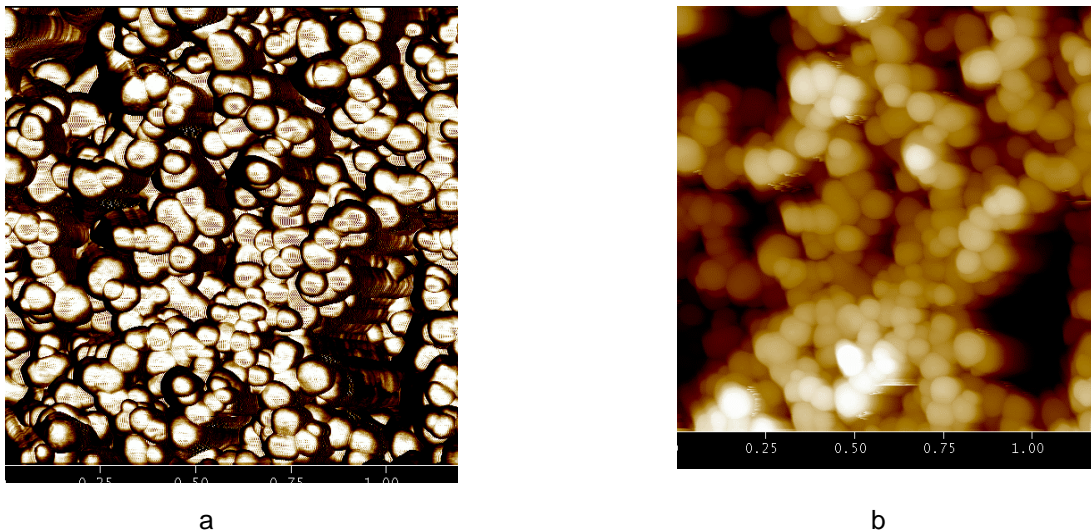

a

b

Figure 15. Atomic Force Micrographs of NAVSEA-IH nano-Al particles (1.25 μ^2 area), With A Uniform, Spherical (~60-70 nm) Morphology: a) Phase Image and b) Height Image.
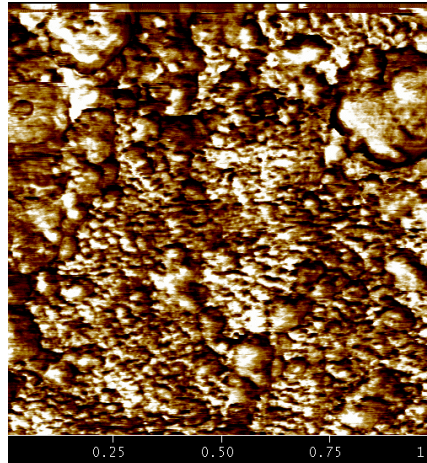
Figure 16. Atomic Force Micrographs (1.25 μ^2 area) of Ultra Fine Al Flake, Showing That Although Sub-Micron Structures are Present, They are Fused Together onto a Much Larger Crystal.

CONCLUSIONS

The results of high resolution imaging of carbon nanotube and nano-Al modifiers for energetic materials have been presented. For the carbon nanotubes, the ultimate goal is to exploit their properties of very high thermal and electrical conductivity, and aspect ratio for initiation and burning rate modification and for enhanced vulnerability properties. Key to this will be the ability to disperse them uniformly into the energetic material matrix. To this end, functionalized carbon nanotubes have been prepared and characterized. The results show that PMMA (in which the polymerization actively occured at the defect site) has been attached at the defect sites of "bamboo" type nanotubes, but that not all of the polymerized PMMA that formed was covalently bonded to the nanotubes. Concepts for incorporating nanocrystalline oxidizers into nanotubes have been performed, which if successful, would also offer potential for improving the vulnerability properties of energetic materials.

Nano-aluminum has been studied in detail in this paper at the atomic level using high-resolution electron microscopy. These results will be combined with theoretical studies in the near future to propose an atomistic model for the surface oxidation. The results are provide fundamental structure information which will serve as a basis for understanding and improving the performance properties and aging characteristics of nano-Al pertinent to the understanding of the role of the aluminum fuel in propellant combustion and as a component of MICs (Metastable Intermolecular Composites) and thermobaric explosives.

ACKNOWLEDGEMENTS

REFERENCES

Berber, S., Kwon, Y., Tomanek, D., "Unusually High Thermal Conductivity of Carbon Nanotubes", Phys. Rev. Lett. 84, 2000.

Bratcher, M. S., Gersten, B. Kosik, W., Ji, H., Mays, J., "A Study in the Dispersion of Carbon Nanotubes", Proceedings of the Materials Research Society Fall 2001 Meeting, in press.

Carnahan, D., Nanolab, Inc., Brighton, MA, www.Nano-Lab.com, personal communication, 2001.

Che, J., Cagin, T., Goddard, W., "Thermal Conductivity of Carbon Nanotubes", http://www.foresight.org/Conferences/MNT7/Papers/Che/index.html

Chen, J., Hamon M.A., Hu, H., Chen, Y.S., Rao, A.M., Eklund, P.C., Haddon, R.C., "Solution Properties of Single-Walled Carbon Nanotubes", Science, 282 (5386): 95-98 Oct. 2, 1998.

Crump, J.E., J.L. Prentice and K.J. Kraeutle, "Role of Scanning Electron Microscope in Study of Solid Propellant Combustion:Behavior of Metal Additives," Combustion Science and Technology, Vol. 1, p.205, 1969.

Dekker, C. "Carbon Nanotubes as Molecular Quantum Wires", Physics Today, p.22, May, 1999.

Ellenbogen, J.C., Love, J.C., "Architectures for Molecular Electronic Computers: 1. Logic Structures and an Adder Built from Molecular Electronic Diodes", Mitre Report, July 1999.

Frank, S., et al., Science 280 1744, 1998.
http://electra.physics.gatech.edu/group/labs/tubelab.html

Gao, G., Cagin, T., Goddard, W., "Energetics, Structure, Mechanical and Vibrational Properties of Single Walled Carbon Nanotubes (SWNT)", 1997.
http://www.wag.caltech.edu/foresight/foresight_2.html

Hone, J., Whitney, M., Zettle, A., Synthetic Metals 103, 2498, 1999.

Hooton, I., Nanopowders -Characterization Studies, Proceedings from DIA New Materials III Symposium, 2-4 April, 2002.

Iijima, S., "Helical microtubules of graphitic carbon" *Nature* **354**, 56-58, 1991.

Kisielowski, C., Hetherington, C.J.D., Wang, Y.C., Kilaas, R., O'Keefe, M.A. and Thust, A., "Imaging columns of the light elements carbon, nitrogen and oxygen at sub-Ångstrom resolution"**,** *Ultramicroscopy* **89**, 4, 243-263, 2001.

Lee, C.J. and Park, J., "Growth and Structure of Carbon Nanotubes Produced by Thermal Chemical Vapor Deposition", Carbon vol. 39, 2001, pp. 1891-1896.

Malm, J.-O. and O'Keefe, M.A., "Deceptive "Lattice Spacings" in High-Resolution Micrographs of Metal Nanoparticles", *Ultramicroscopy* **68**, 13-23, 1997.

O'Keefe, M.A., Buseck, P.R. and Iijima, S., "Computed crystal structure images for high resolution electron microscopy", *Nature* **274,** 322-324, 1978.

O'Keefe, M.A., Hetherington, C.J.D., Wang, Y.C., Nelson, E.C., Turner, J.H., Kisielowski, C., Malm, J.-O., Mueller, R., Ringnalda, J., Pan, M. and Thust, A., "Sub-Ångstrom High-Resolution Transmission Electron Microscopy at 300keV"**,** *Ultramicroscopy* **89,** 4, 215-241, 2001.

O'Keefe, M.A., Nelson, E.C. and Allard, L.F., "Focal-Series Reconstruction of Nanoparticle Exit-Surface Electron Wave", *Microscopy & Microanalysis* **9**, 2: 278-279, 2003.

Pan, Z.W., Sie, S.S., Chang, B.H., Wang, C.Y., Lu, L., Liu, W., Zhou, W.Y., Li, W.Z., Qian, L.X., Nature, 394 6694, p.631-632, 1998.

Price, E.W. "Combustion of Metallized Particles", Chapter 9 from "Fundamentals of Solid-Propellant Combustion", Edited by K. Kuo and M.Summerfield, Progress in Astronautics and Aeronautics, Vol. 90, p. 479, 1984.

Sanvito, S., Kwon, Y,. Tomanek, D., Lambert, C., "Fractional Quantum Conductance in Carbon Nanotubes", Phys. Rev. Lett. 84, 1974.

Schewe, P.F., Stein. B., "Physics News Update, The American Institute of Physics Bulletin of Physics News, Number 279 (Story#2), 15 July. 1996.
http://www.aip.org/enews/physnews/1996/split/pnu279-2.htm

Wilder, J.W.,G., Venema, L.C., Rinzler, A.G., Smalley, R.E., Dekker, C., Nature 391, 6662, 59-62, 1998.

Yakobson, B. I., Smalley, R. E., "Fullerene Nanotubes: C(1,000,000) and Beyond," American Scientist, 85 p324-337, 1997 (see also references therein).

Witt, W.Z., Naturforsch. A, 1967, 22A, 92.

Yu M.F. et al. Phys. Rev. Lett. 84, 5552, 2000.

Zarko, V.E. "Metal Combustion in Rockets", Chapter 10 from "Modelling and Performance Prediction in Rockets and Guns", Edited by S.R. Chakravarthy, S. Krishnan, Allied Publishers Limited, P.301, 1998.